Synthesis of isoprene atmospheric oxidation products: isomeric epoxydiols and the rearrangement products *cis- and trans-3-methyl-3,4-dihydroxytetrahydrofuran*

Zhenfa Zhang, Ying-Hsuan Lin, Haofei Zhang, Jason D. Surratt, Louise M. Ball, Avram Gold

Department of Environmental Sciences and Engineering, Gillings School of Global Public Health, The University of North Carolina at Chapel Hill, NC, USA

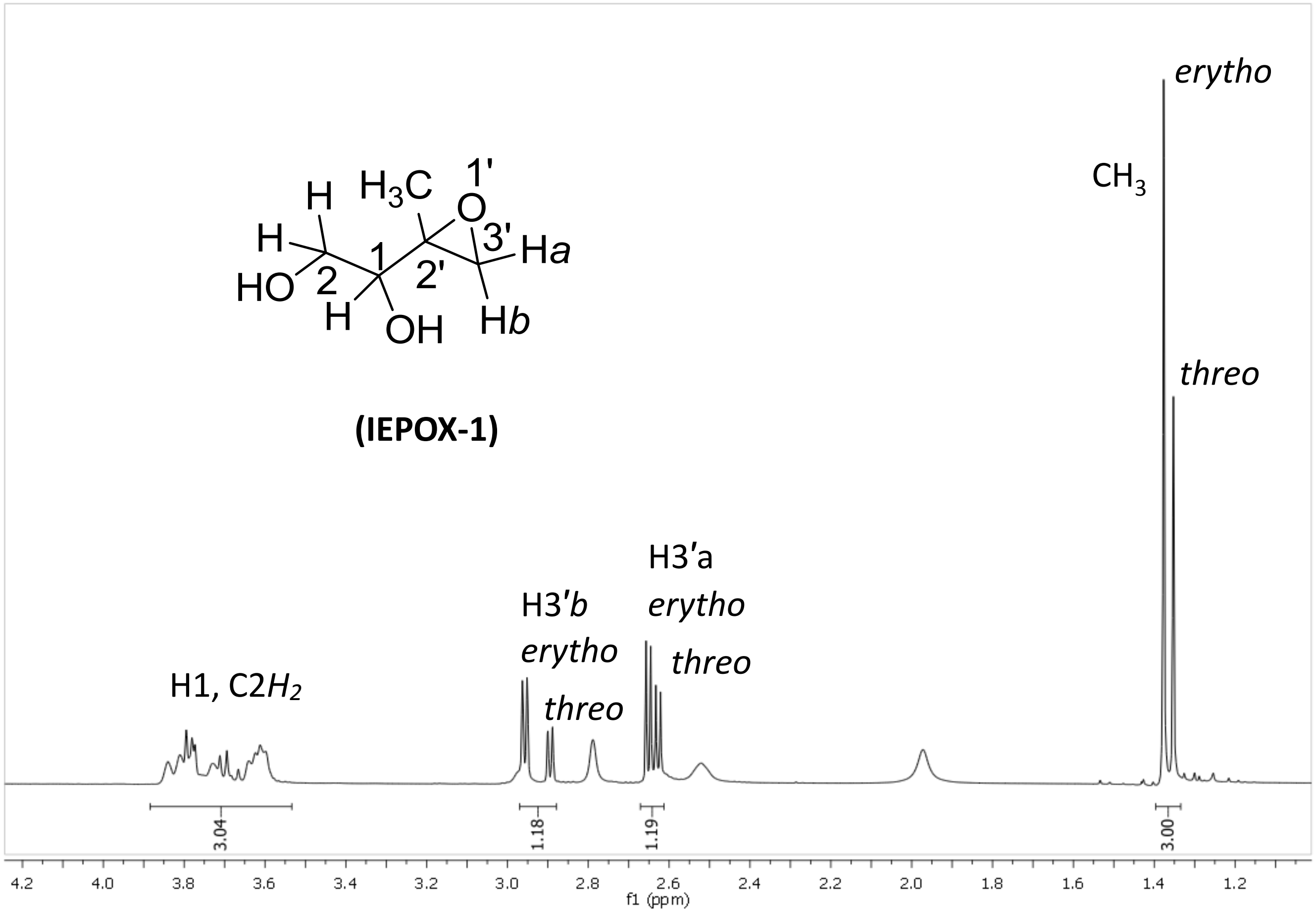

Figure S1. ^{1}H NMR (400 MHz, $CDCl_3$) of *erythro*- and *threo*-1-(2-methyloxiran-2-yl)ethane-1,2-diol (**IEPOX-1**). The signal for the epoxy ring proton *cis* to the methine hydroxy group ($3'H_b$) in *erythro* isomer is shifted significantly downfield relative to that of the *threo* isomer, in accord with the observation for structural analogs [Adam, *J. Am. Chem. Soc.* **1993**, *115*, 7226.]. The assignment of the *erythro* diastereomer as the major product is consistent with the assignment based on the ^{13}C chemical shifts (see ^{13}C NMR, Figure S2).

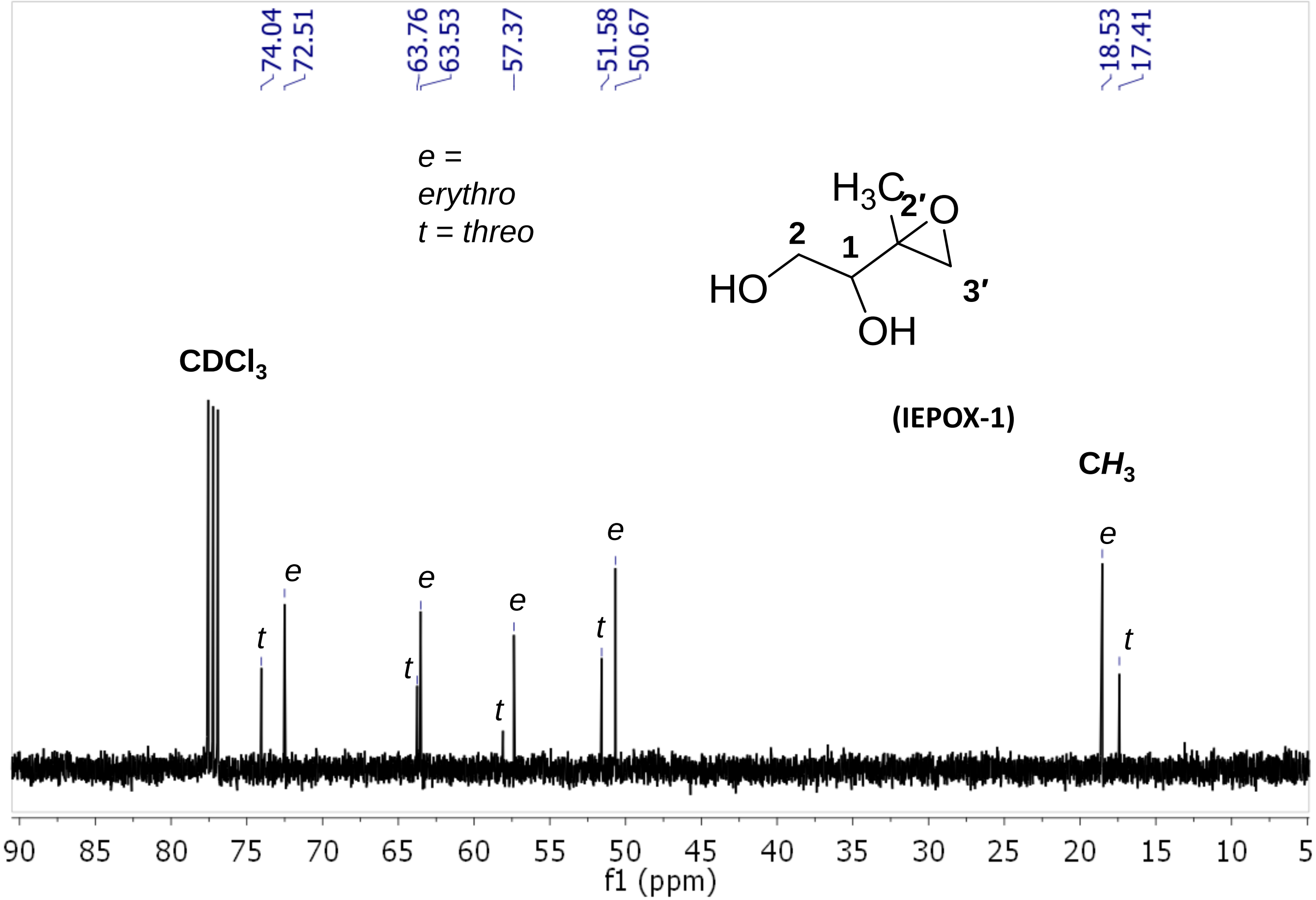

Figure S2. ^{13}C NMR (100 MHz, $CDCl_3$) of *erythro*- and *threo*-1-(2-methyloxiran-2-yl)ethane-1,2-diol (**IEPOX-1**). The distinction between *threo* and *erythro* diastereomers is based on the observation that the chemical shift of all oxygen-bearing carbon atoms of the *erythro* diastereomers are 0.1-3.4 ppm upfield relative to those of the corresponding *threo* diastereomers [Adam JOC 1997]. Of the two sets of signals, the set having upfield chemical shifts for all oxygen-bearing carbons is consequently assigned to the *erythro* diastereomer, which is the major product, and the second set is assigned to the minor *threo* diastereomer.

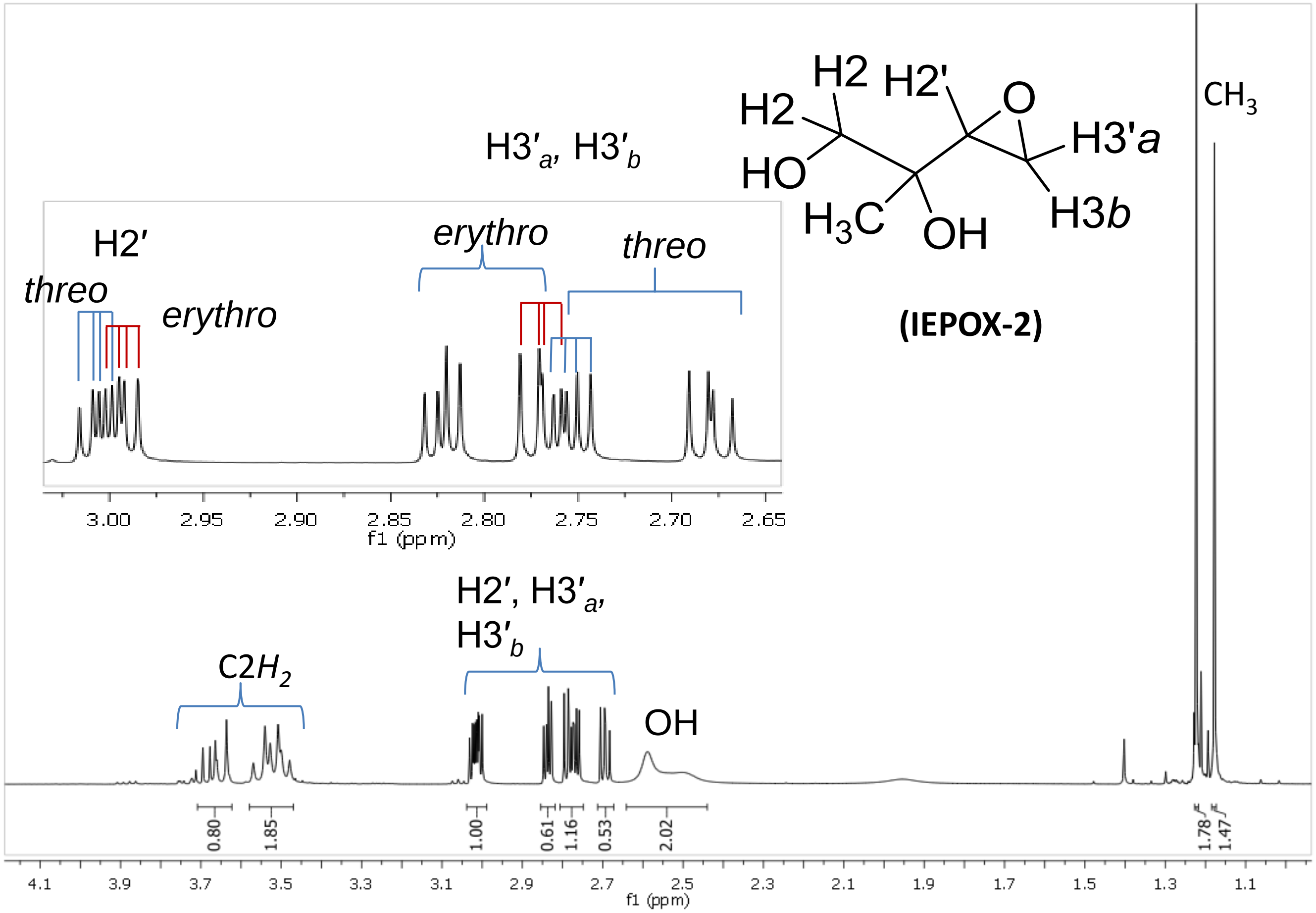

Figure S3. ^{1}H NMR (400 MHz, $CDCl_3$) of 2-(oxiran-2-yl)propane-1,2-diol (**IEPOX-2**). Assignments of signals to *erythro* and *threo* diastereomers is tentative based on the NMR spectrum of the close structural analog linalool epoxide for which the absolute stereochemistry has been established. [a). Morales, C. P.; Catalan, J.; Domingo, V.; Delgado, J. A. G.; Dobado, J. A.; Herrador, M. M.; del Moral, J. F. Q.; Barrero, A. F. *J. Org. Chem*. **2011**, 76, 2494. b). Khomenko, T.M.; Tatarova, L. E.; Korchagina, D. V.; Barkhash, V. A.. *Russ. J. Org. Chem*. **2002**,. 38, 4983].

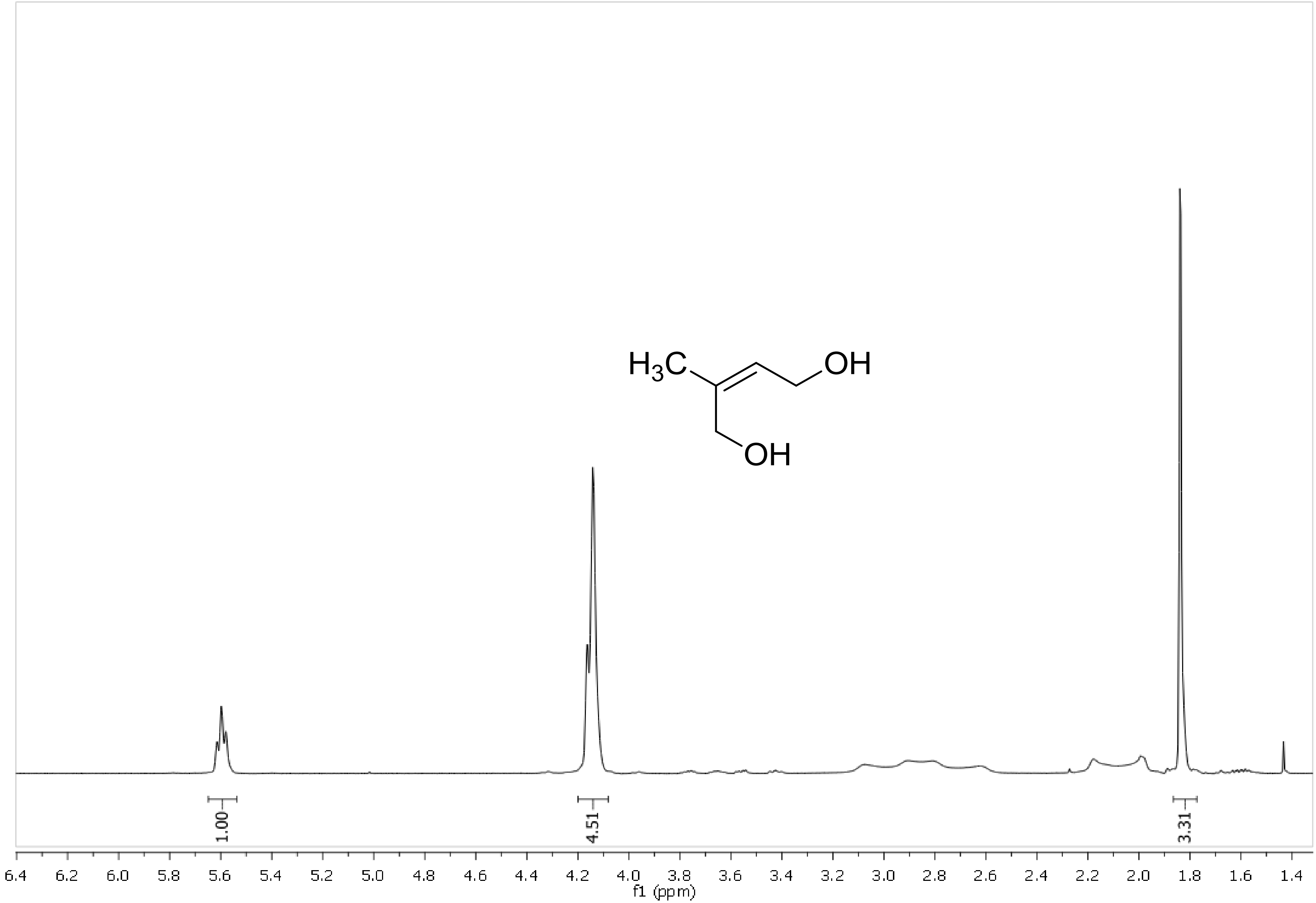

Figure S4. ^{1}H NMR (400 MHz, $CDCl_3$) of (Z)-2-methylbut-2-ene-1,4-diol (**8**).

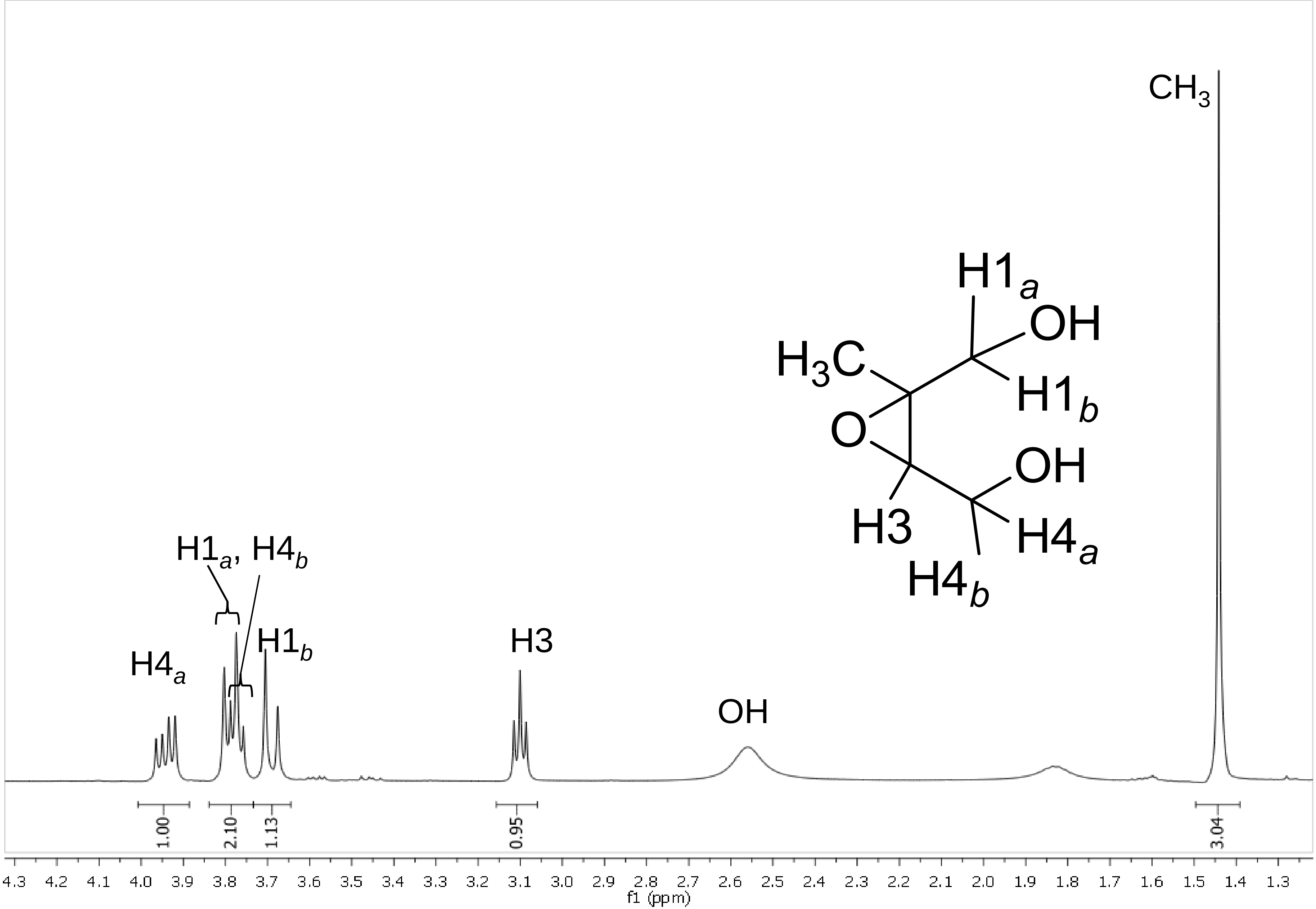

Figure S5. ^{1}H NMR (400 MHz, $CDCl_3$) of *cis*-2-methyl-2,3-epoxybutane-1,4-diol (**IEPOX-3**).

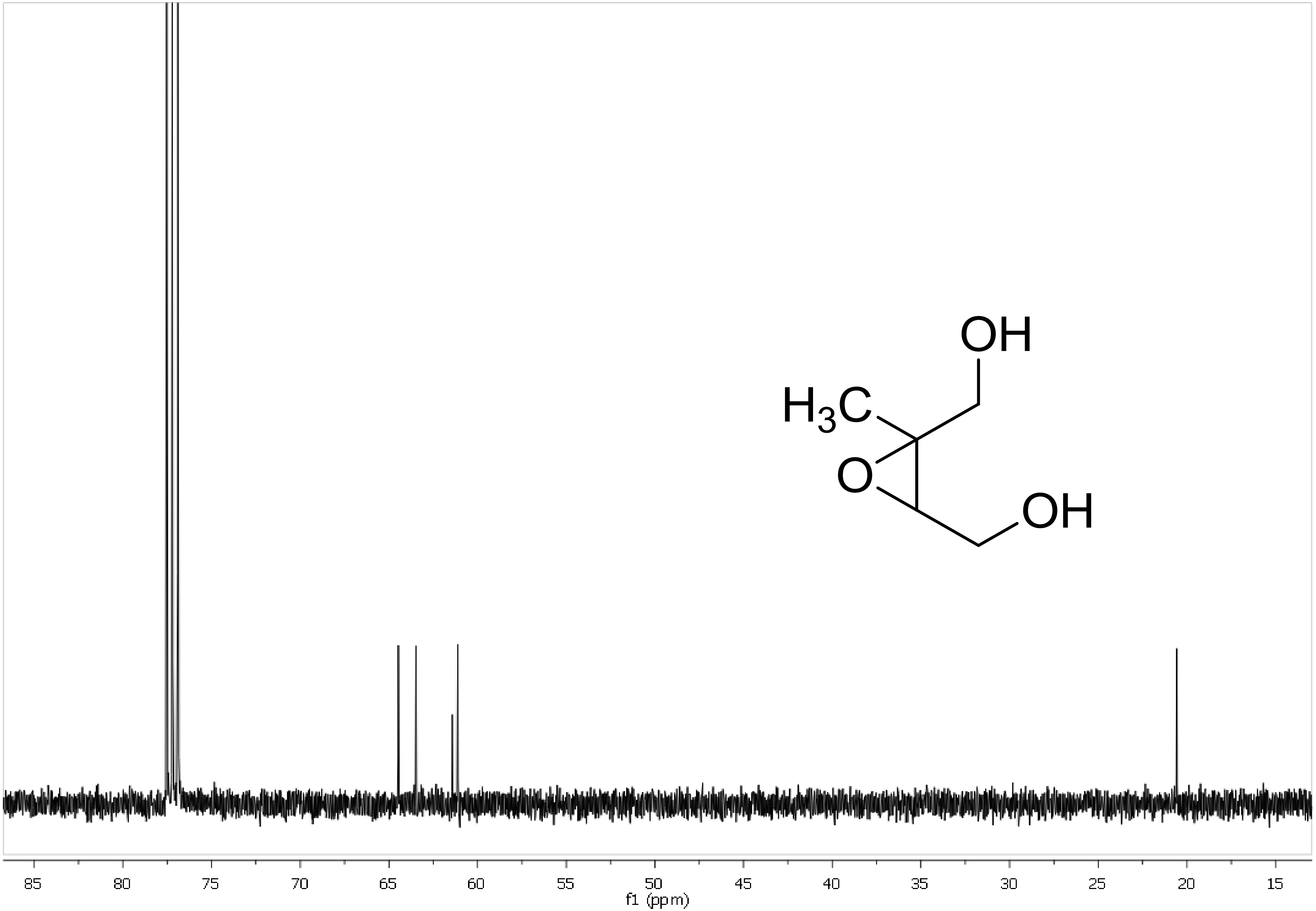

Figure S6. ^{13}C NMR (100 MHz, $CDCl_3$) of *cis*-(2-methyloxirane-2,3-diyl)dimethanol (**IEPOX-3**).

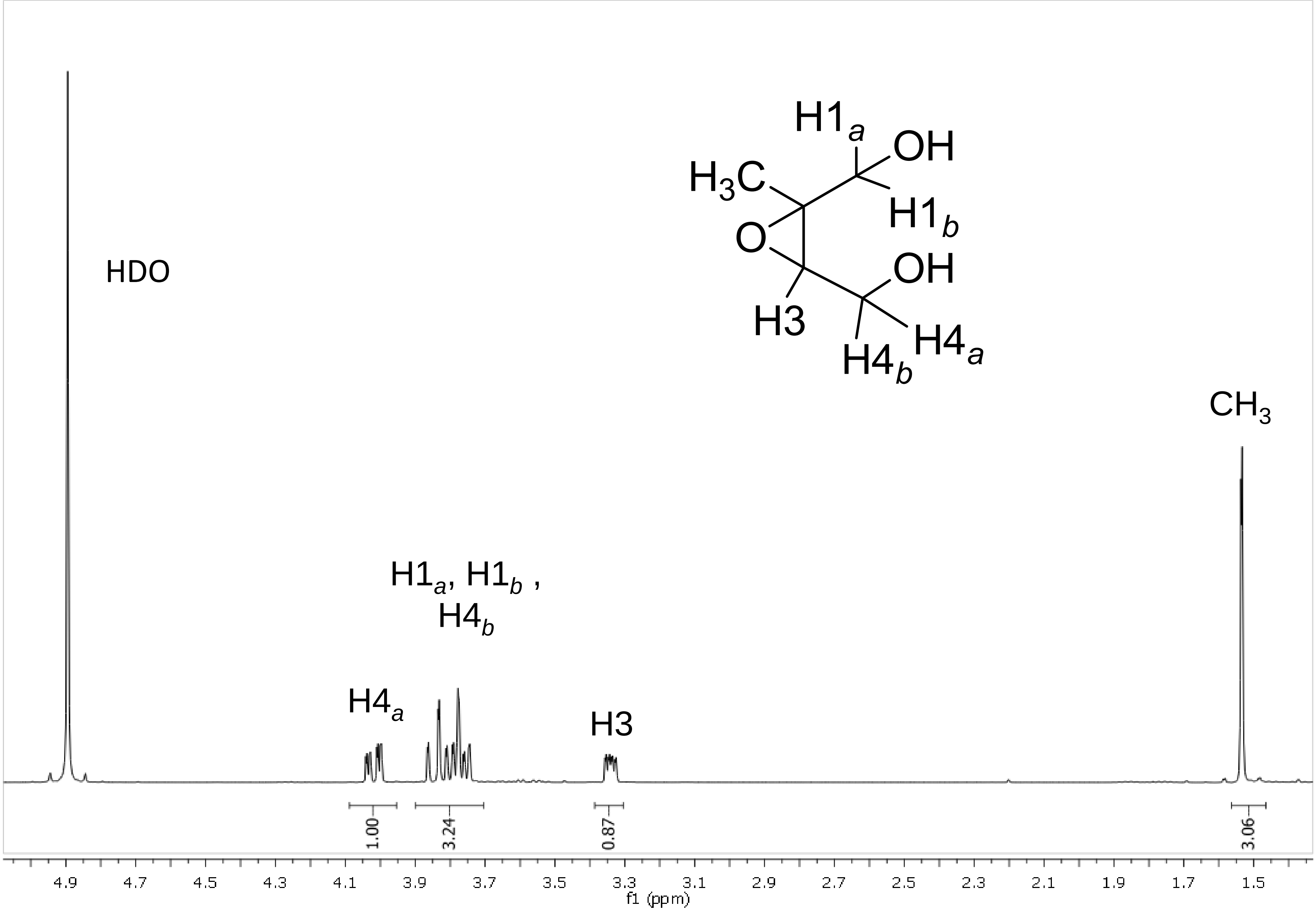

Figure S7. ^{1}H NMR (400 MHz, D_2O) of *cis*-2-methyl-2,3-epoxybutane-1,4-diol (**IEPOX-3**).

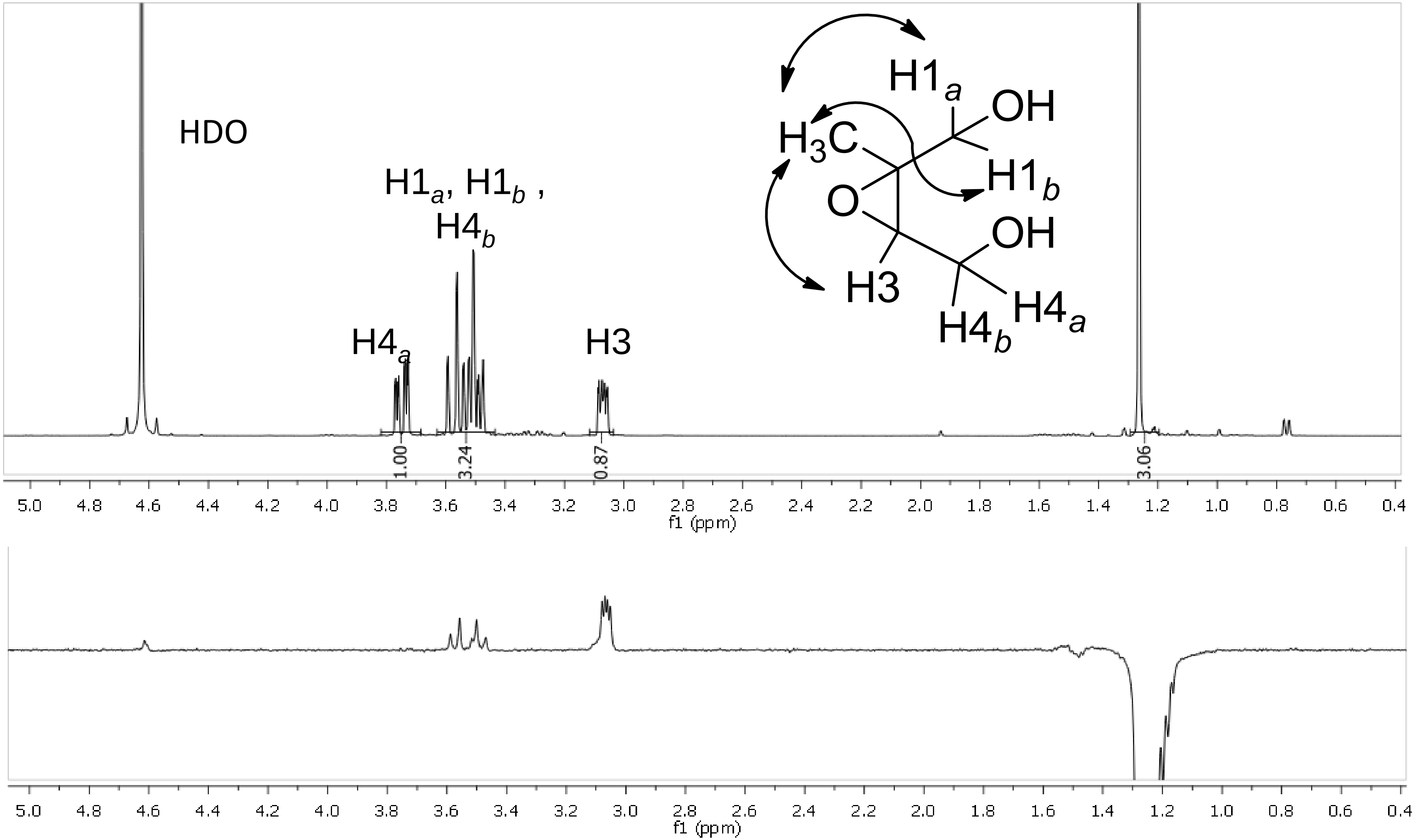

Figure S8. ^{1}H and NOESY 1D NMR (400 MHz, D_2O) of *cis*-2-methyl-2,3-epoxybutane-1,4-diol (**IEPOX-3**). The *cis* geometry of IEPOX-3 is confirmed by strong dipolar coupling between the methyl group and the oxirane proton H3 the 1D NOESY spectrum.

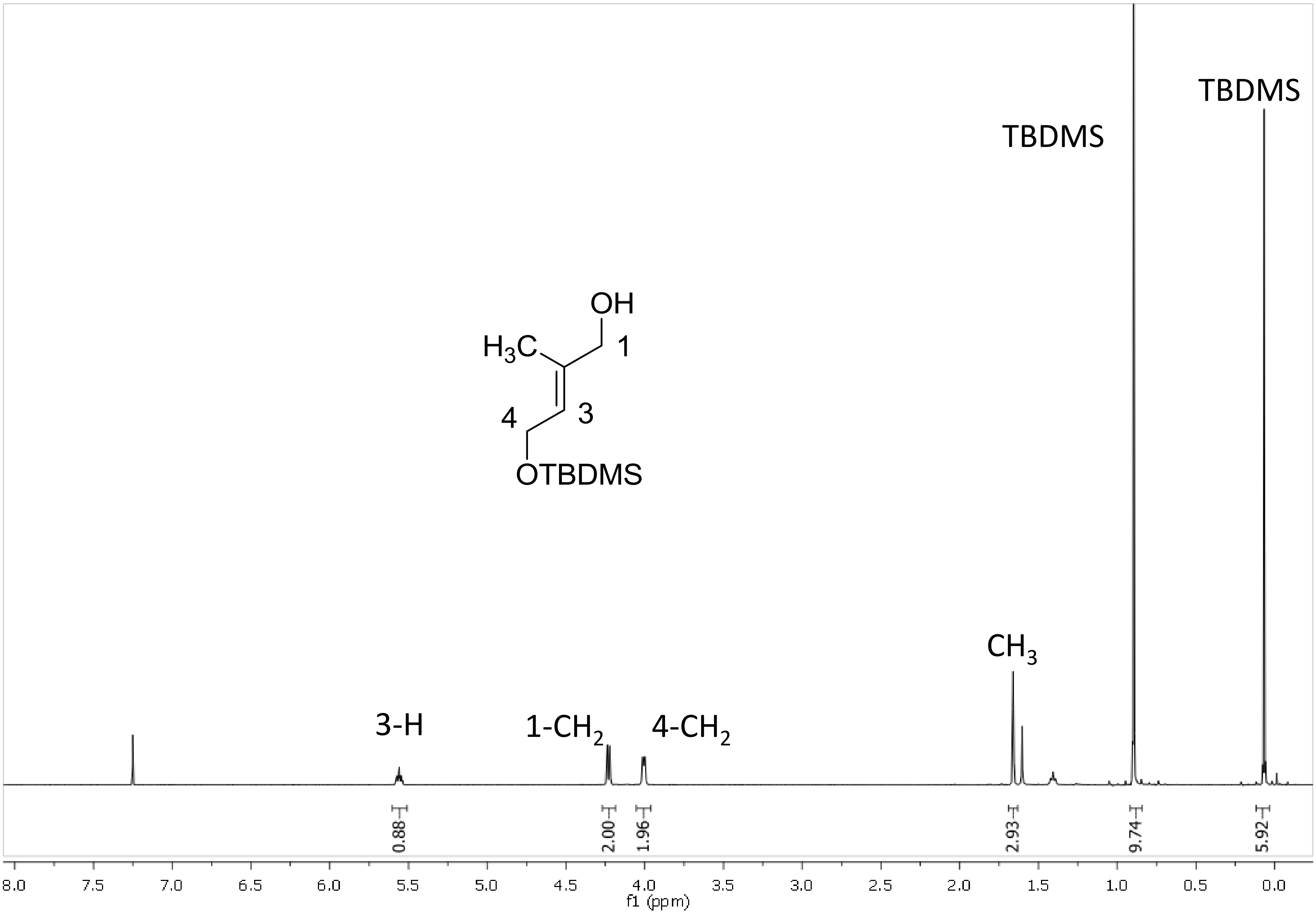

Figure S9. ^{1}H NMR (400 MHz, CDCl$_3$) of *trans*-4-((*tert*-butyldimethylsilyl)oxy)-2-methyl-2-buten-1-ol (**11**).

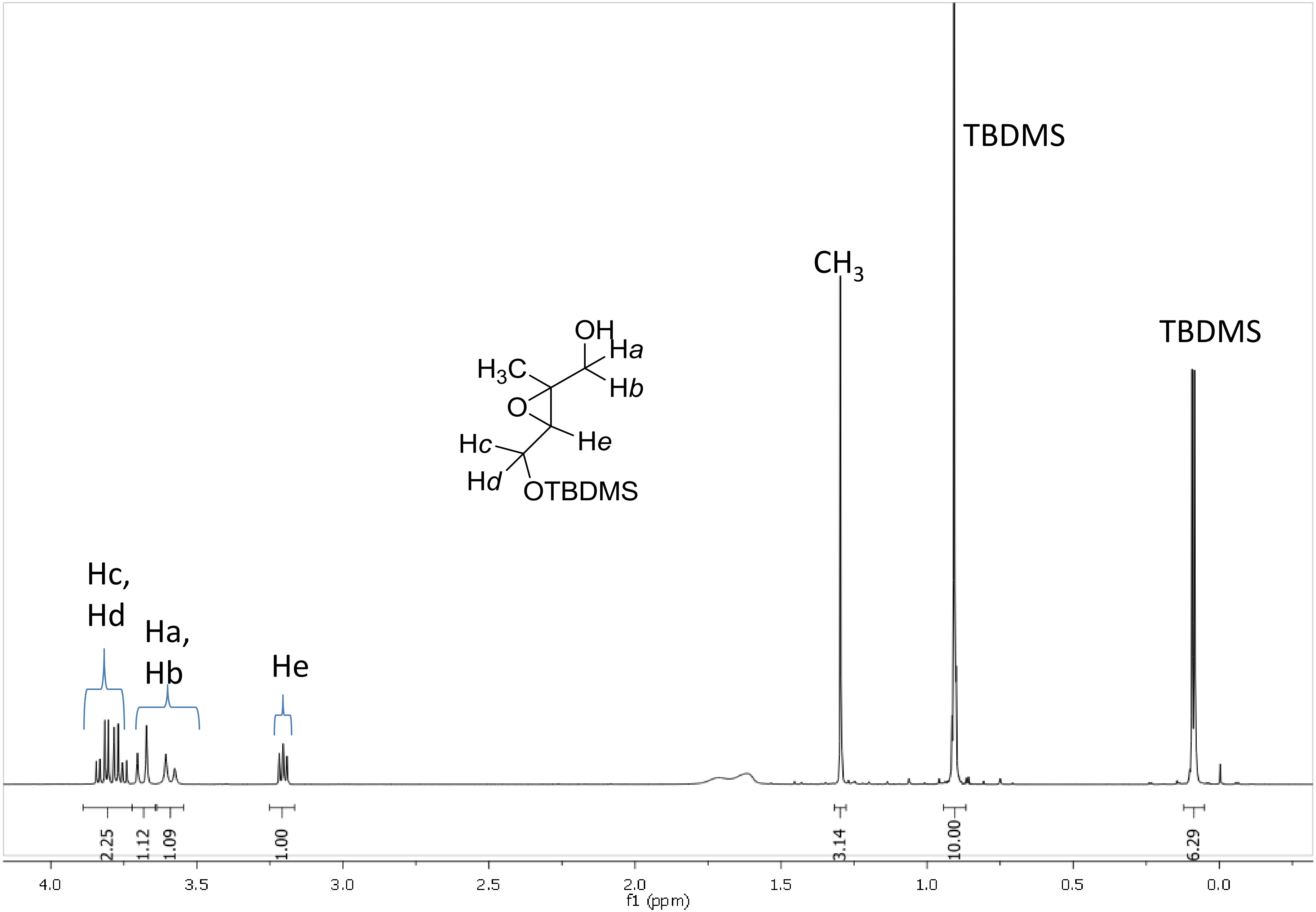

Figure S10. ^{1}H NMR (400 MHz, $CDCl_3$) of (3-(((*tert*-butyldimethylsilyl)oxy)methyl)-2-methyloxiran-2-yl)methanol (**12**).

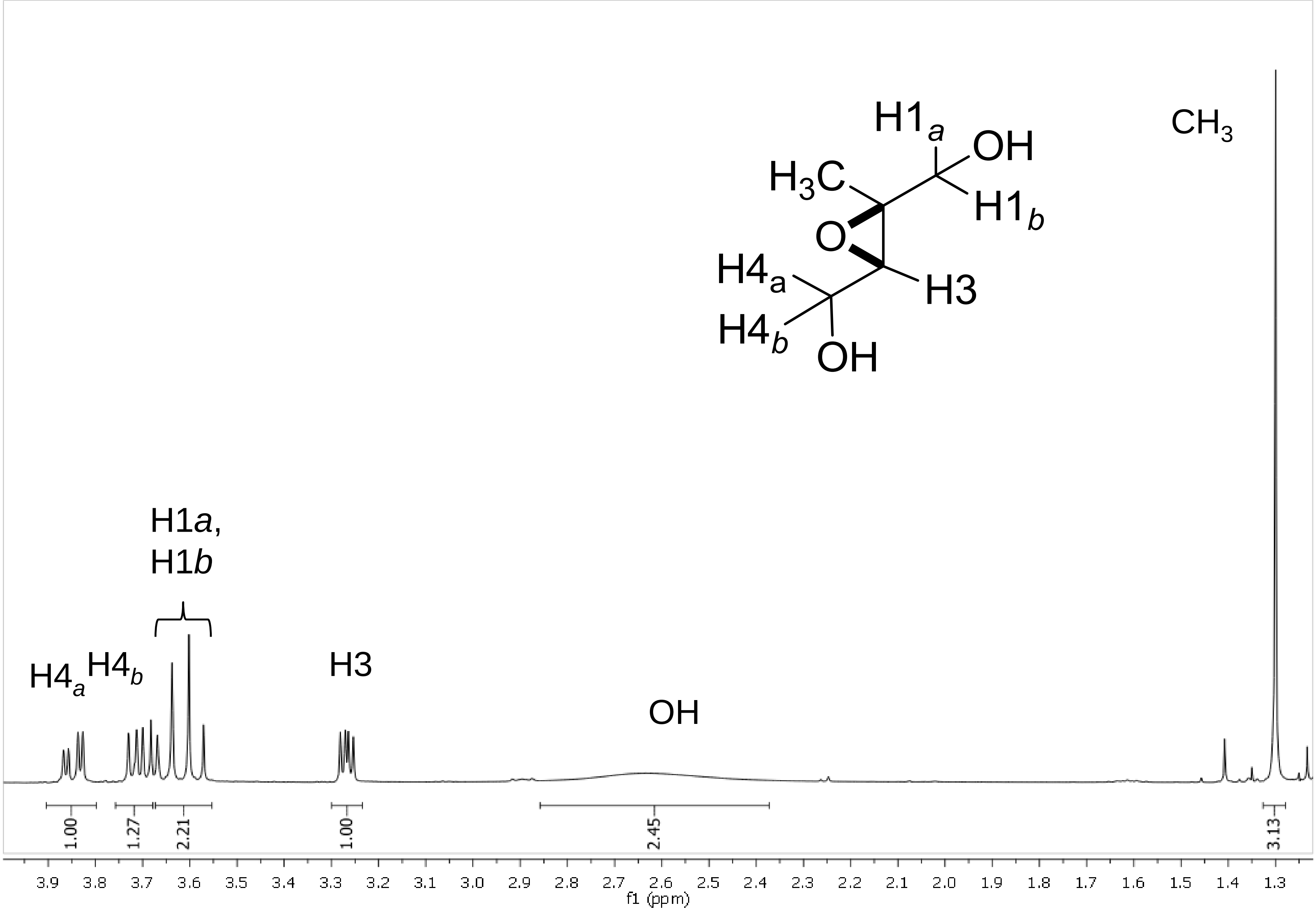

Figure S11. ^{1}H NMR (400 MHz, $CDCl_3$) of *trans*-2-methyl-2,3-epoxybutane-1,4-diol (**IEPOX-4**).

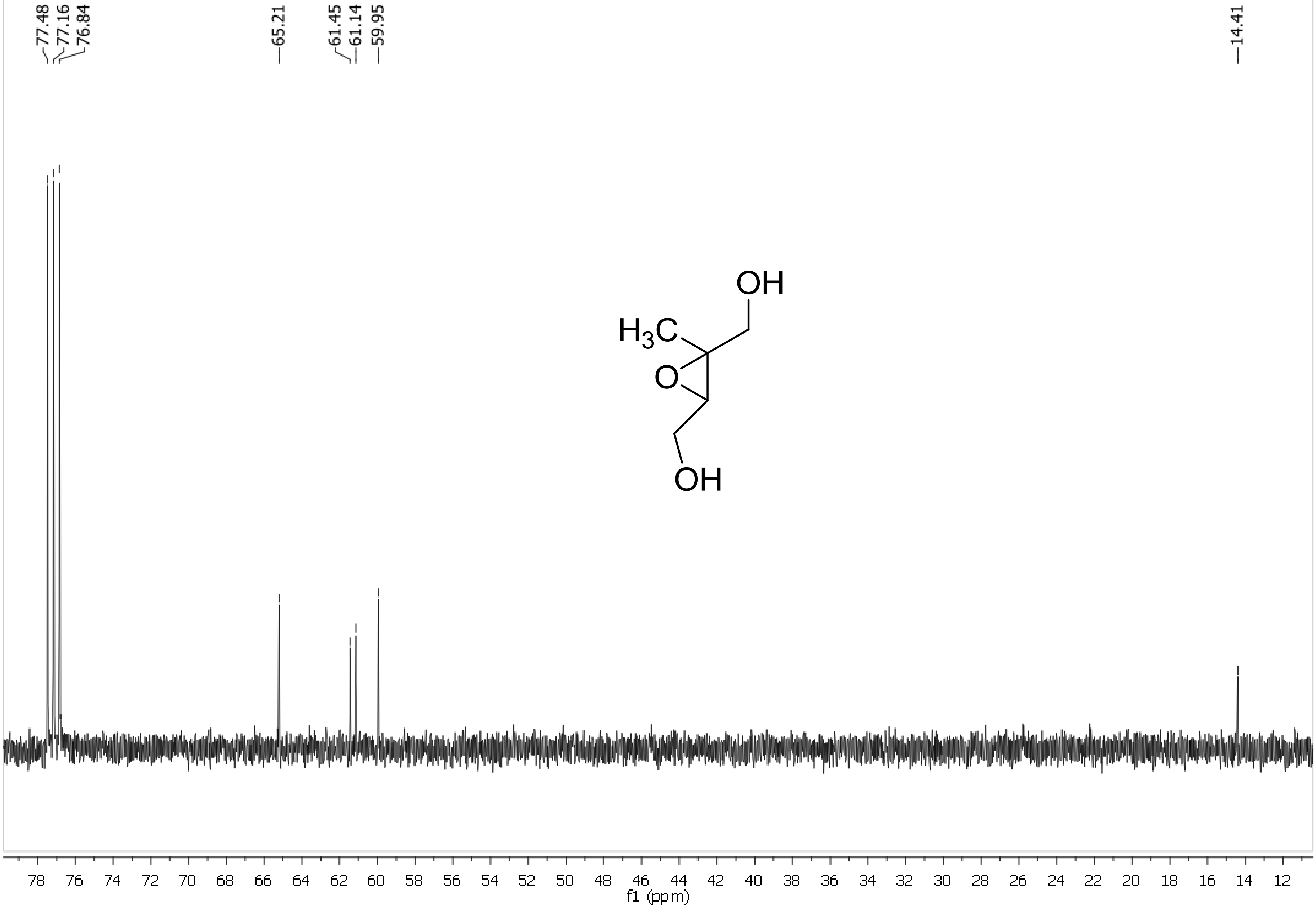

Figure S12. ^{13}C NMR (100 MHz, $CDCl_3$) of *trans*-2-methyl-2,3-epoxybutane-1,4-diol (**IEPOX-4**).

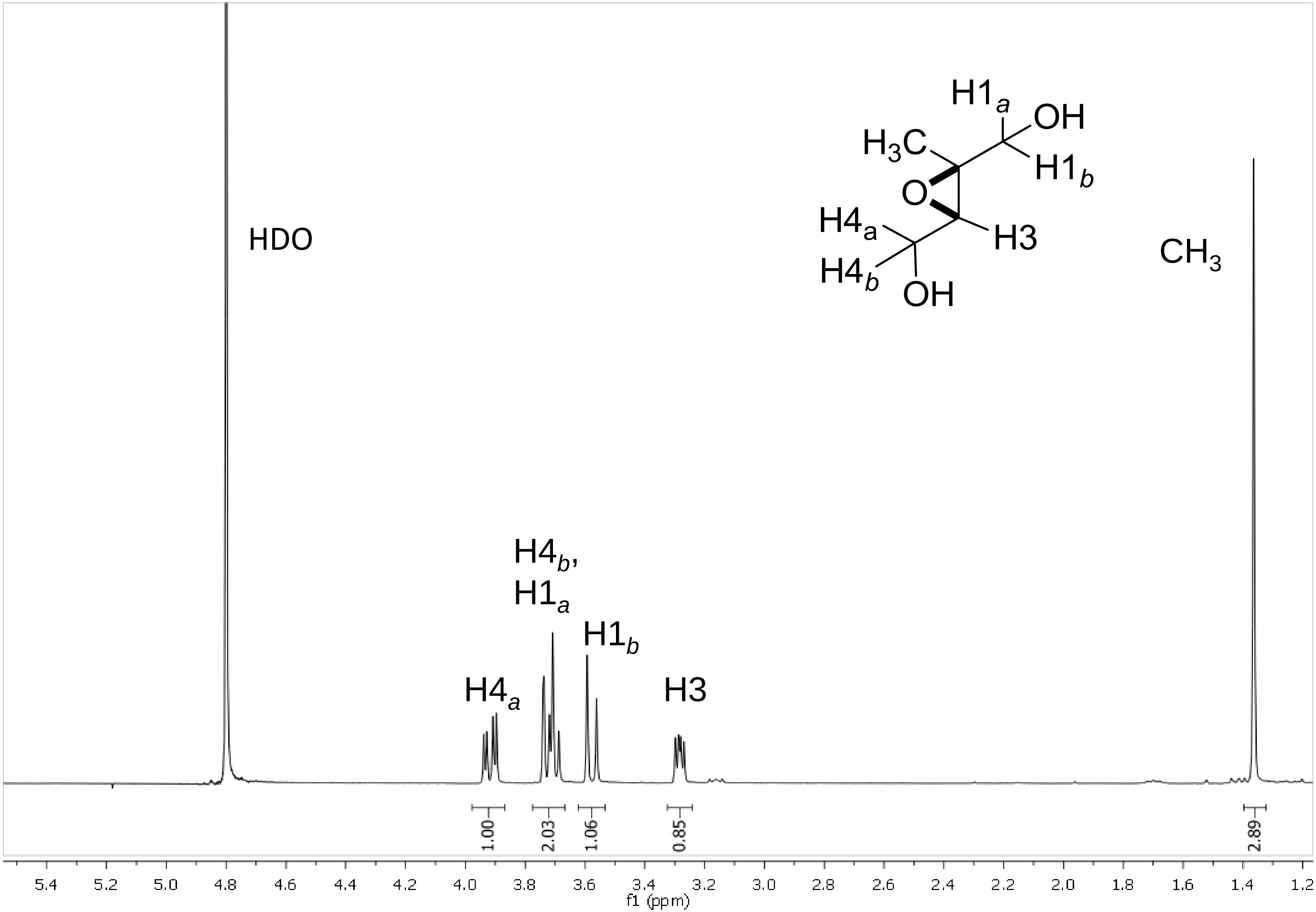

Figure S13. ^{1}H NMR (400 MHz, D_2O) of *trans*-2-methyl-2,3-epoxybutane-1,4-diol (**IEPOX-4**).

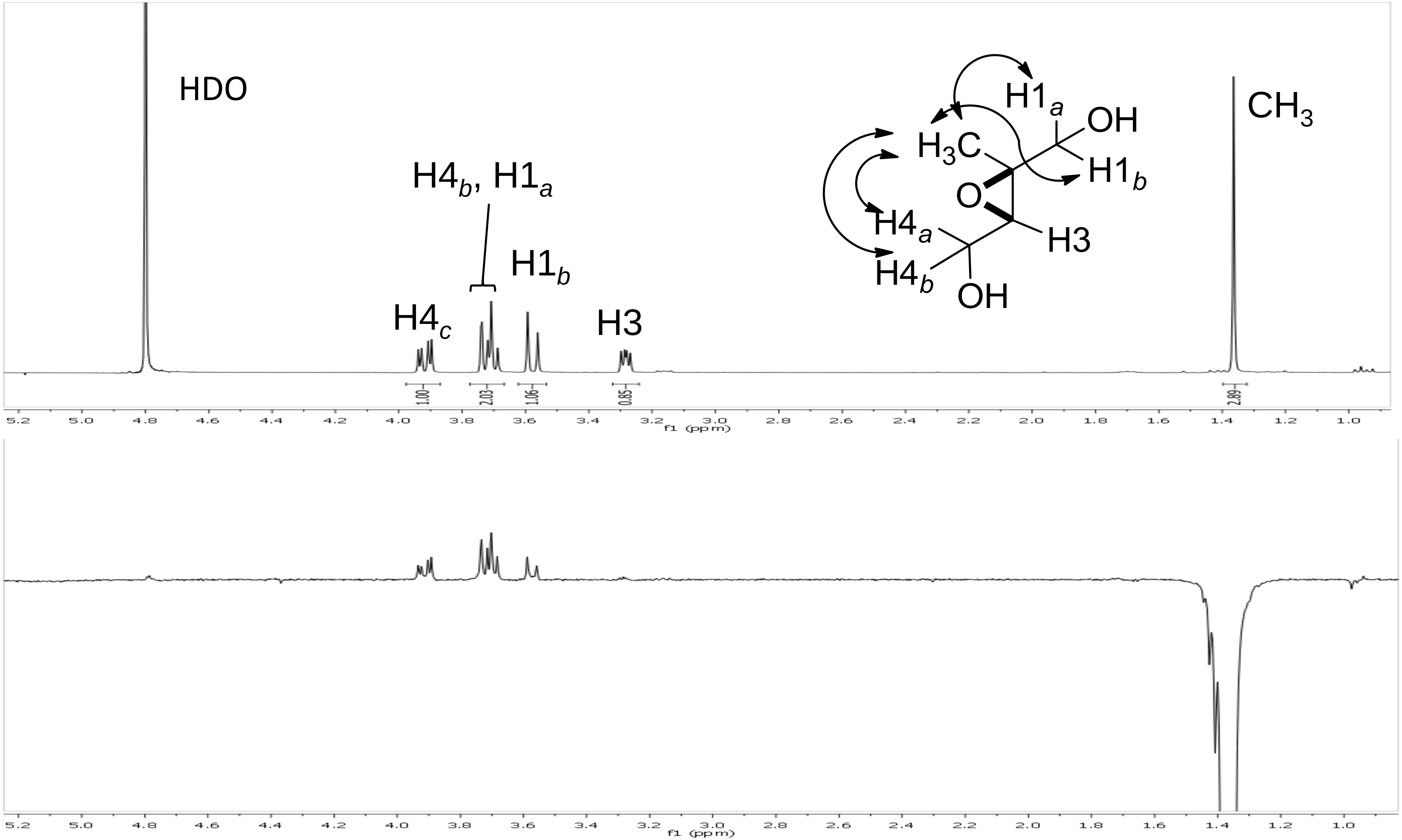

Figure S14. ^1H and NOESY 1D NMR (400 MHz, D_2O) of *trans*-2-methyl-2,3-epoxybutane-1,4-diol (**IEPOX-4**). The *trans*-configuration is confirmed by the absence of an NOE correlation between the methyl group and oxirane proton H3 in the 1D NOESY spectrum.

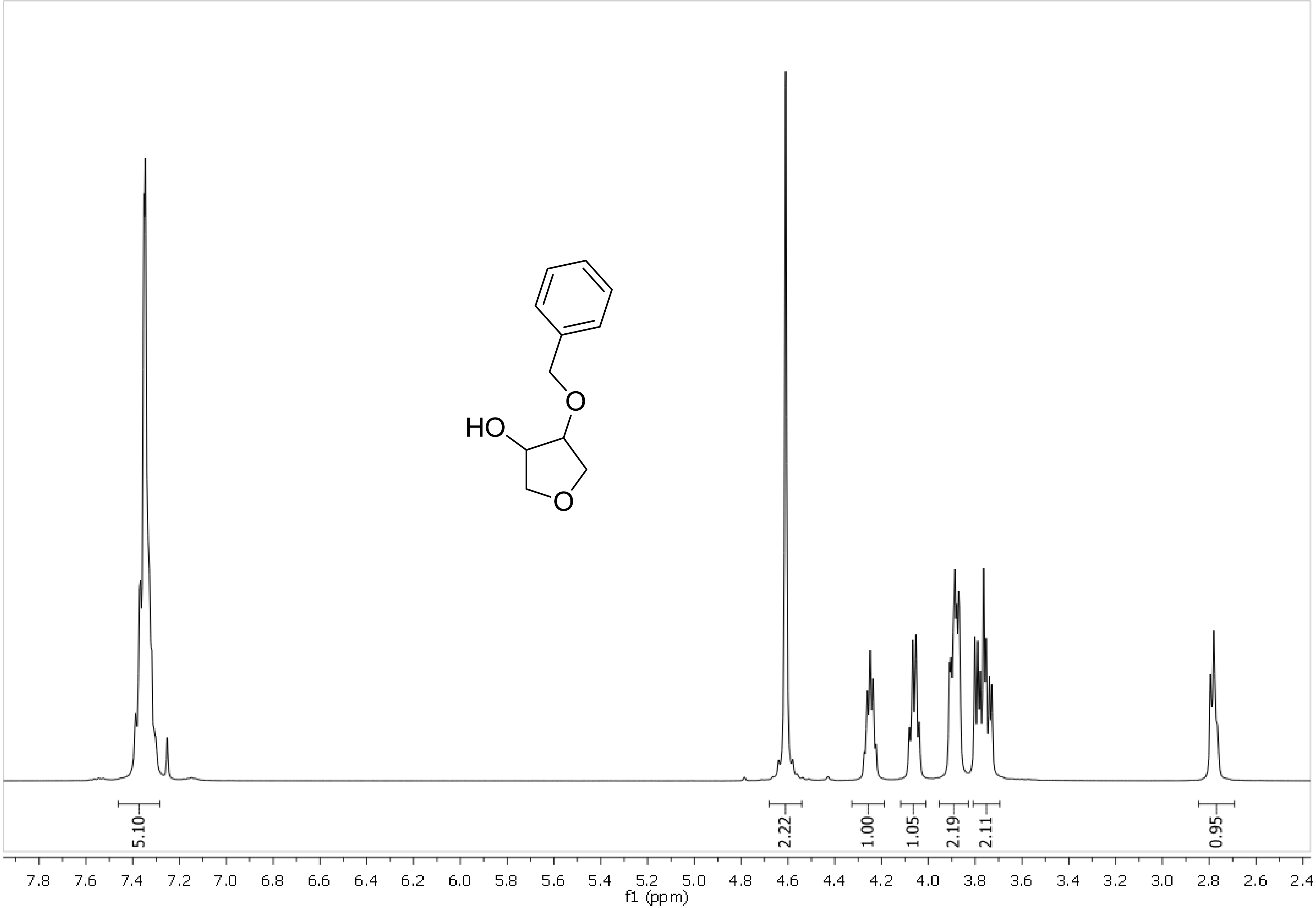

Figure S15. ^{1}H NMR (400 MHz, $CDCl_3$) of 4-(benzyloxy)tetrahydrofuran-3-ol (**17**).

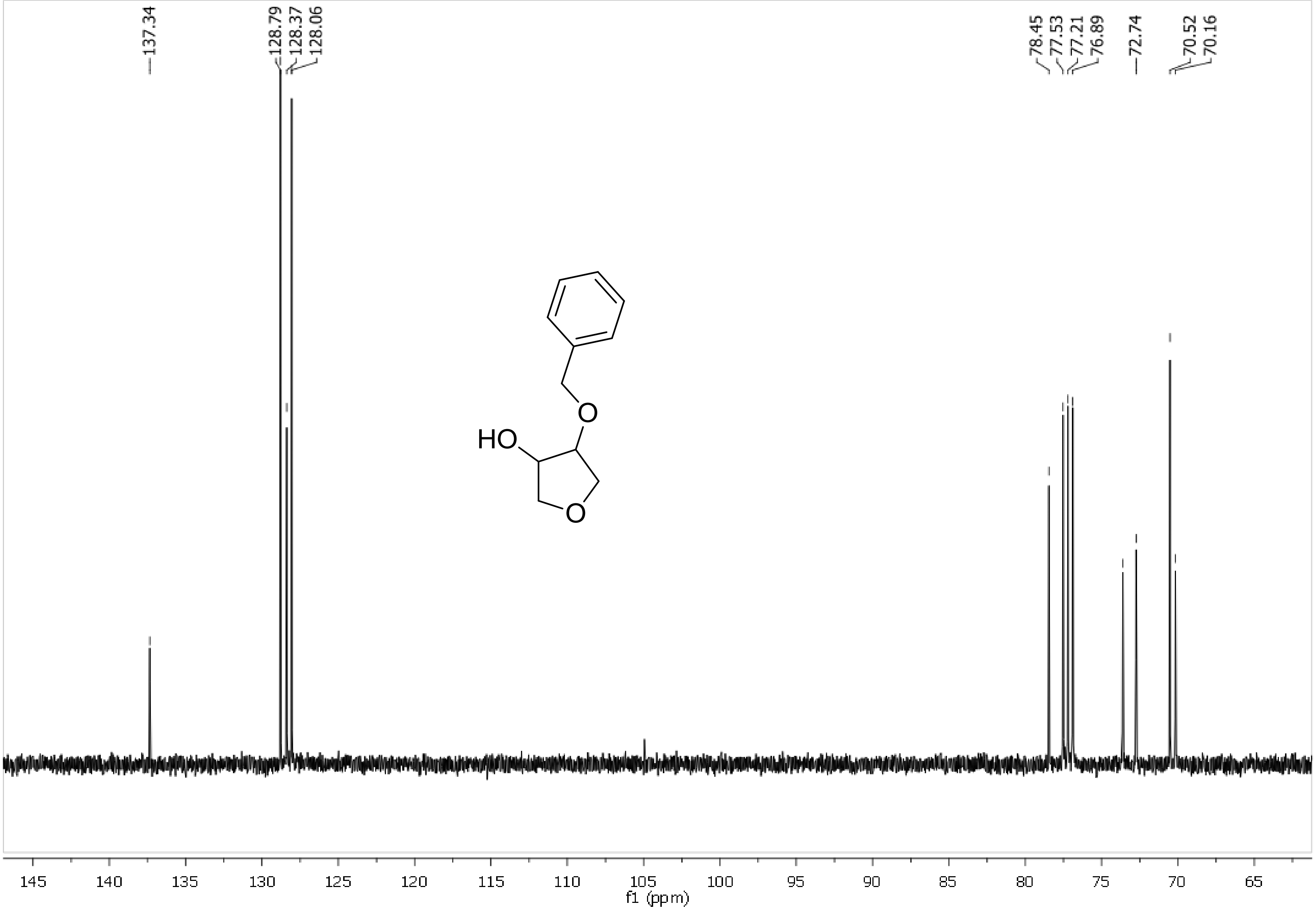

Figure S16. ^{13}C NMR (100 MHz, $CDCl_3$) of 4-(benzyloxy)tetrahydrofuran-3-ol (**17**).

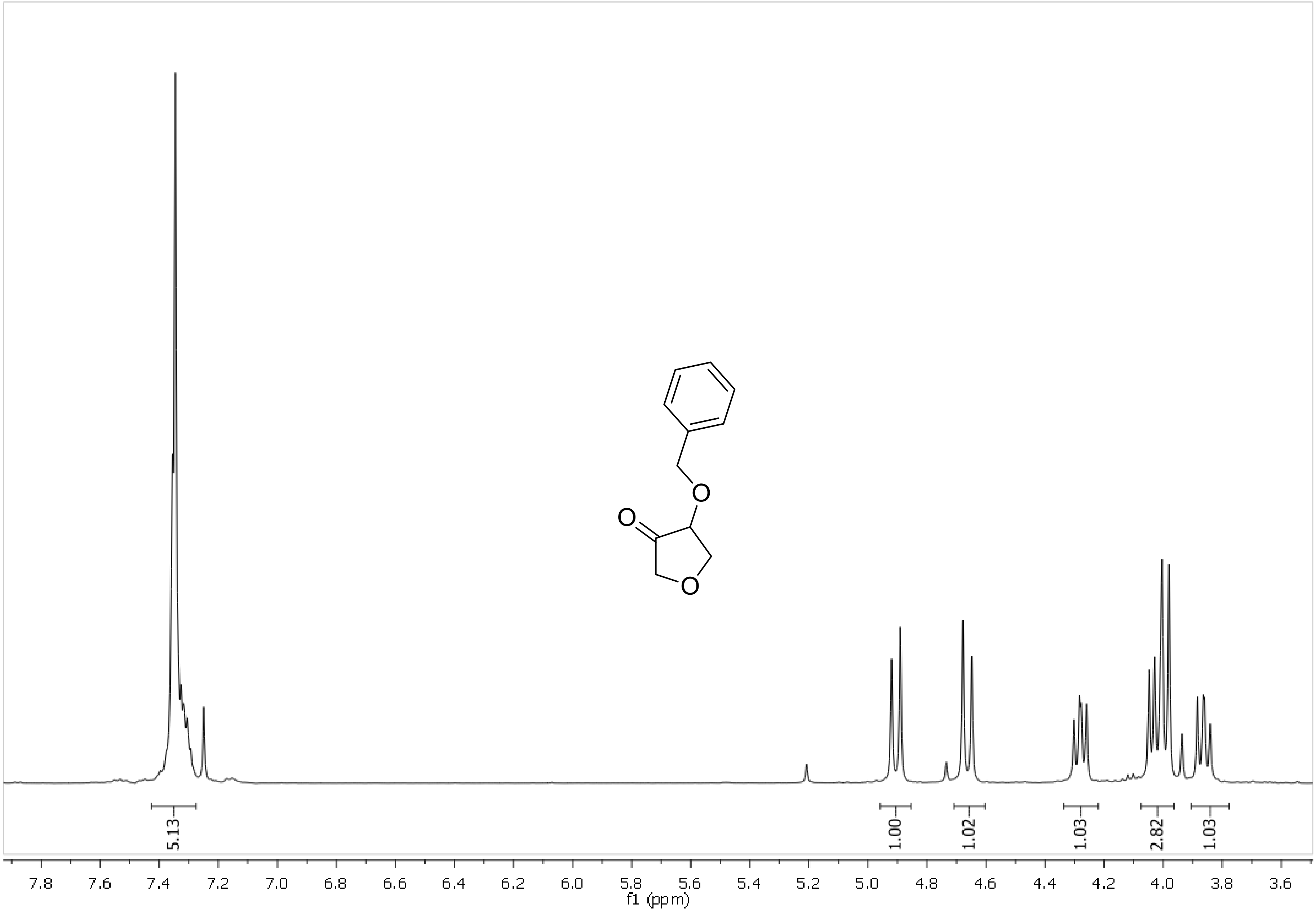

Figure S17. ^{1}H NMR (400 MHz, $CDCl_3$) of 4-(benzyloxy)dihydrofuran-3(2*H*)-one (**18**).

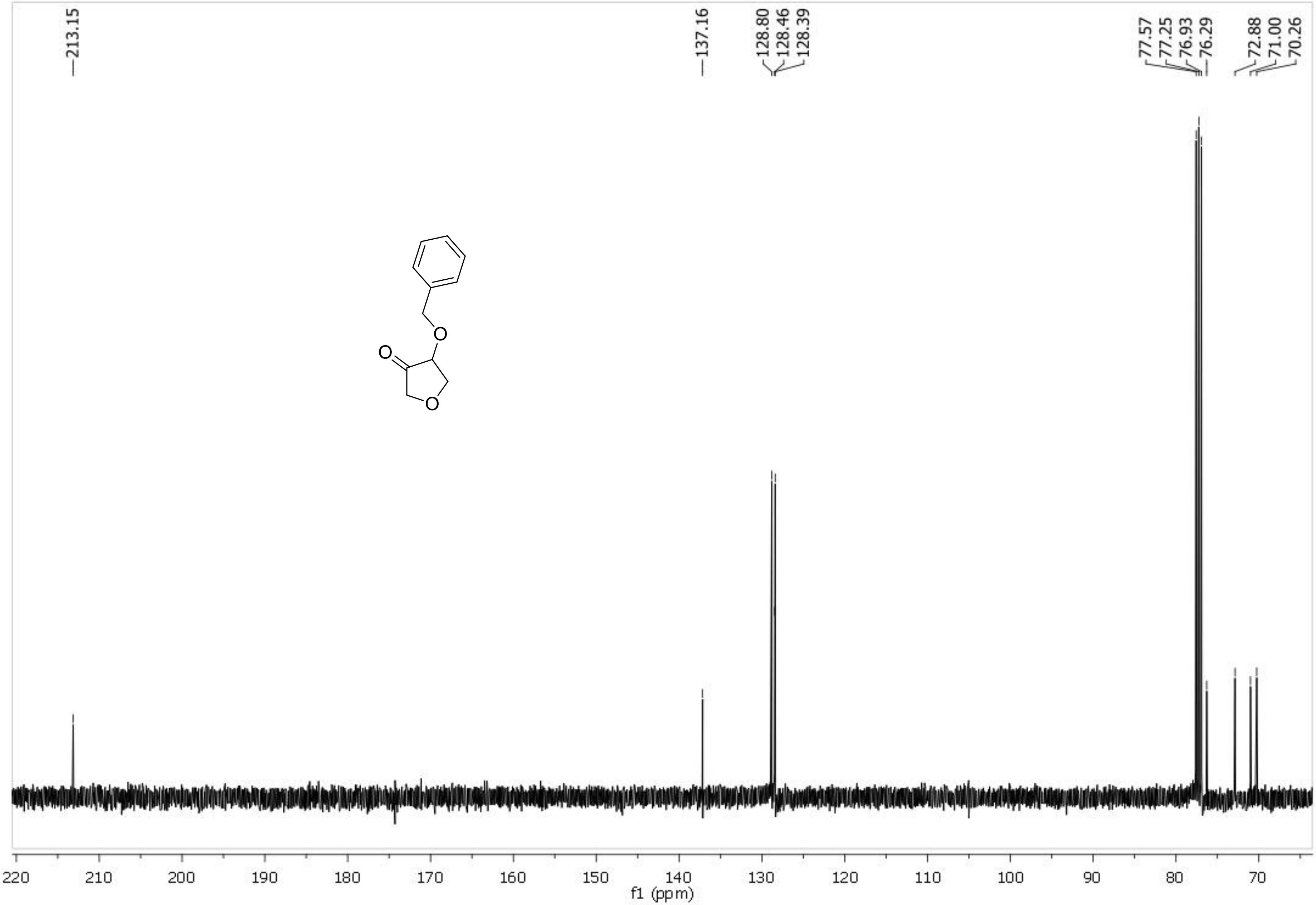

Figure S18. ^{13}C NMR (100 MHz, $CDCl_3$) of 4-(benzyloxy)dihydrofuran-3(2*H*)-one (**18**).

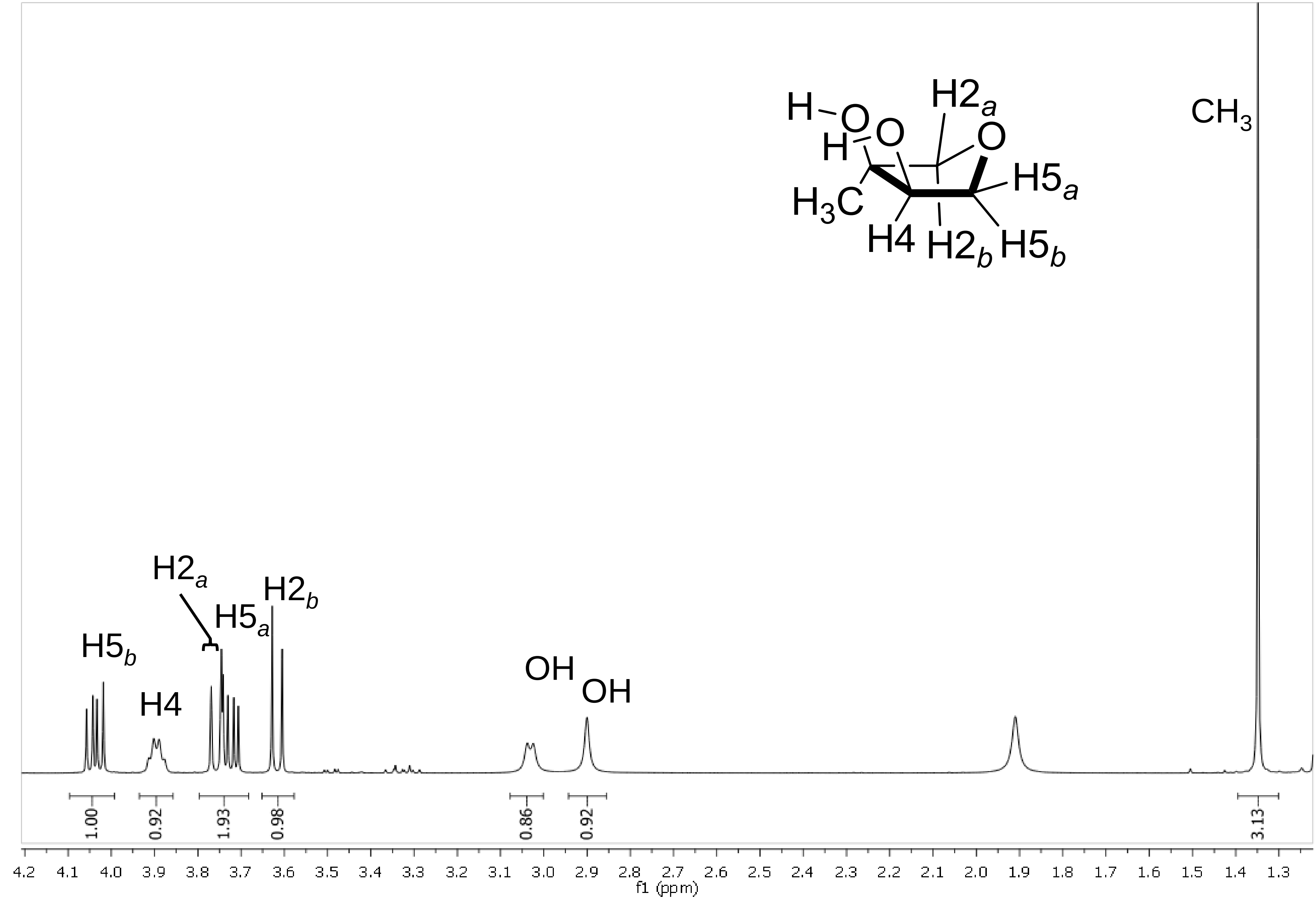

Figure S19. ^{1}H NMR (400 MHz, CDCl$_3$) of *cis*-3-methyltetrahydrofuran-3,4-diol (**14**).

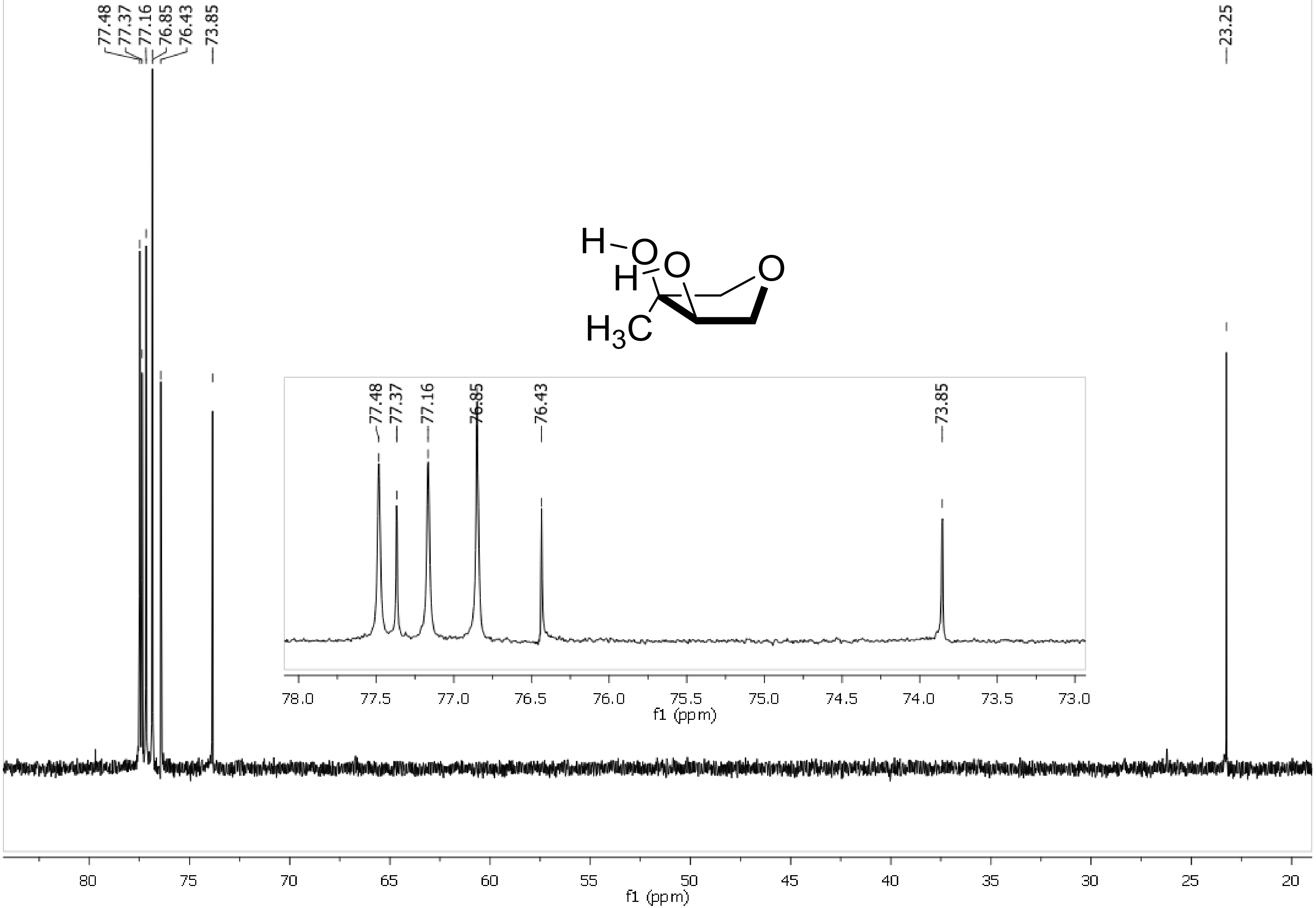

Figure S20. ^{13}C NMR (100 MHz, $CDCl_3$) of *cis*-3-methyltetrahydrofuran-3,4-diol (**14**).

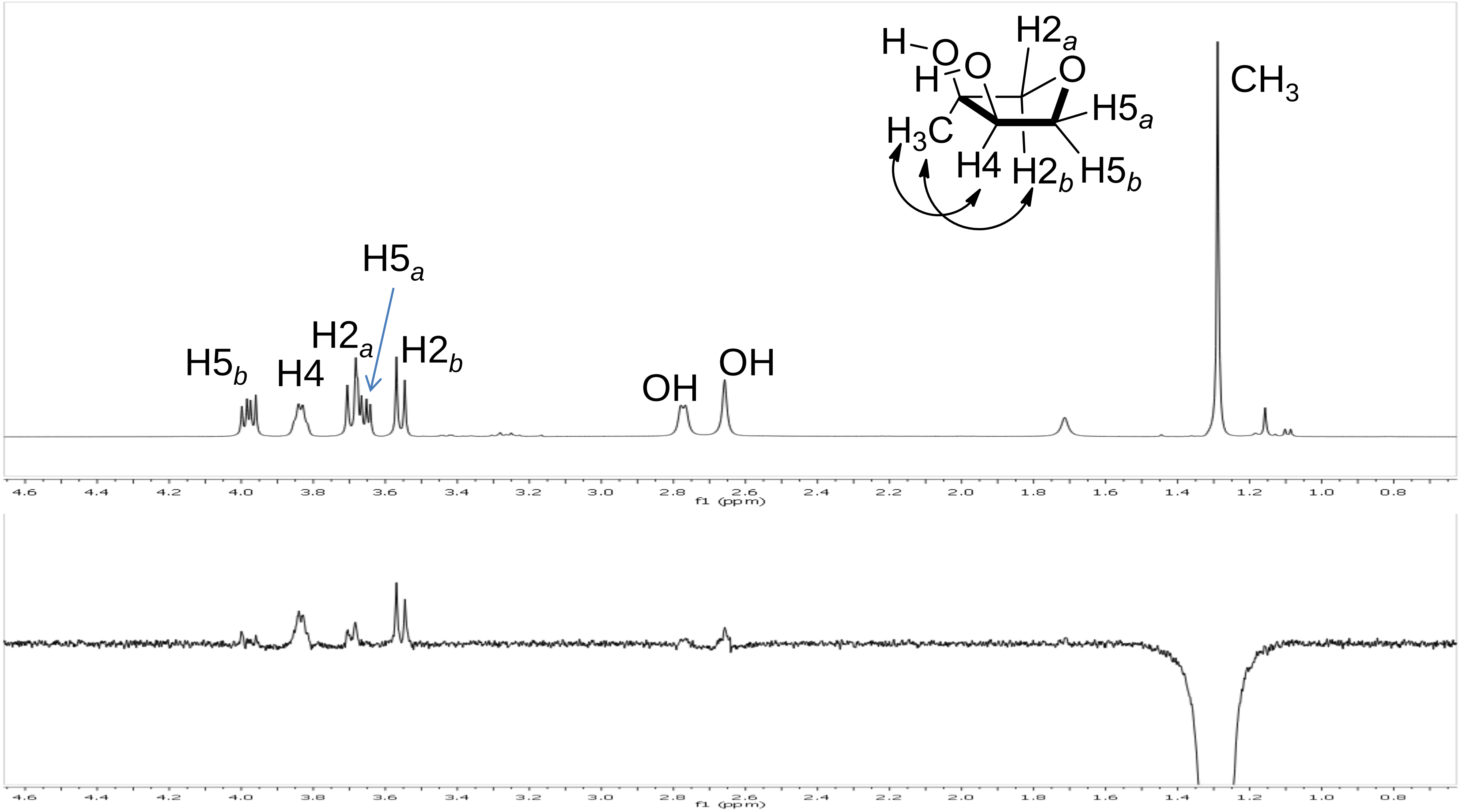

Figure S21. ^{1}H and NOESY 1D NMR (400 MHz, $CDCl_3$) of *cis*-3-methyltetrahydrofuran-3,4-diol (**14**). In the 1D NOESY spectrum, strong enhancement of the signal for carbinyl H4 on irradiation of the neighboring 3-methyl signal confirms the *cis*-isomeric structure.

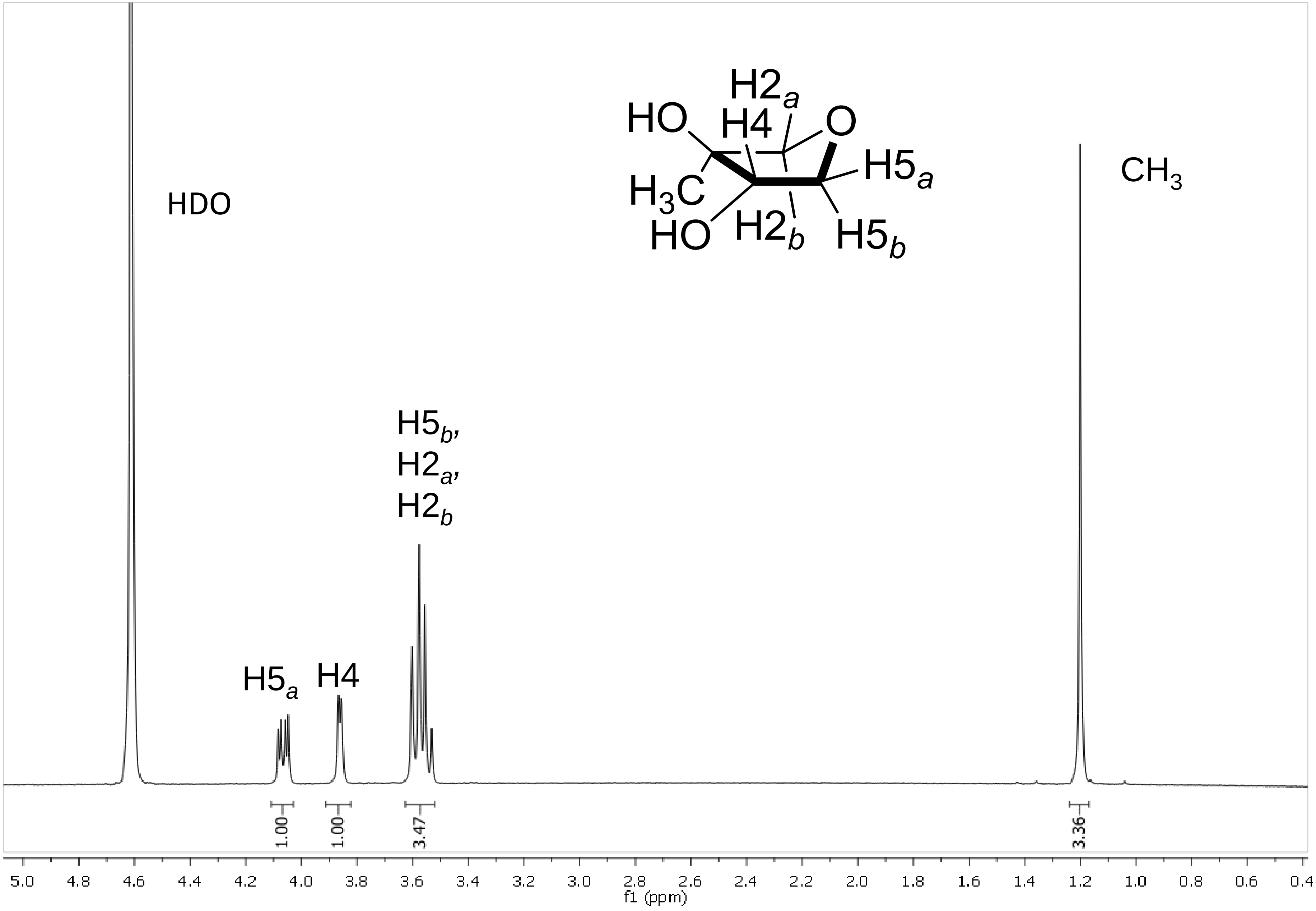

Figure S22. ^{1}H NMR (400 MHz, D_2O) of *trans*-3-methyltetrahydrofuran-3,4-diol (**15**).

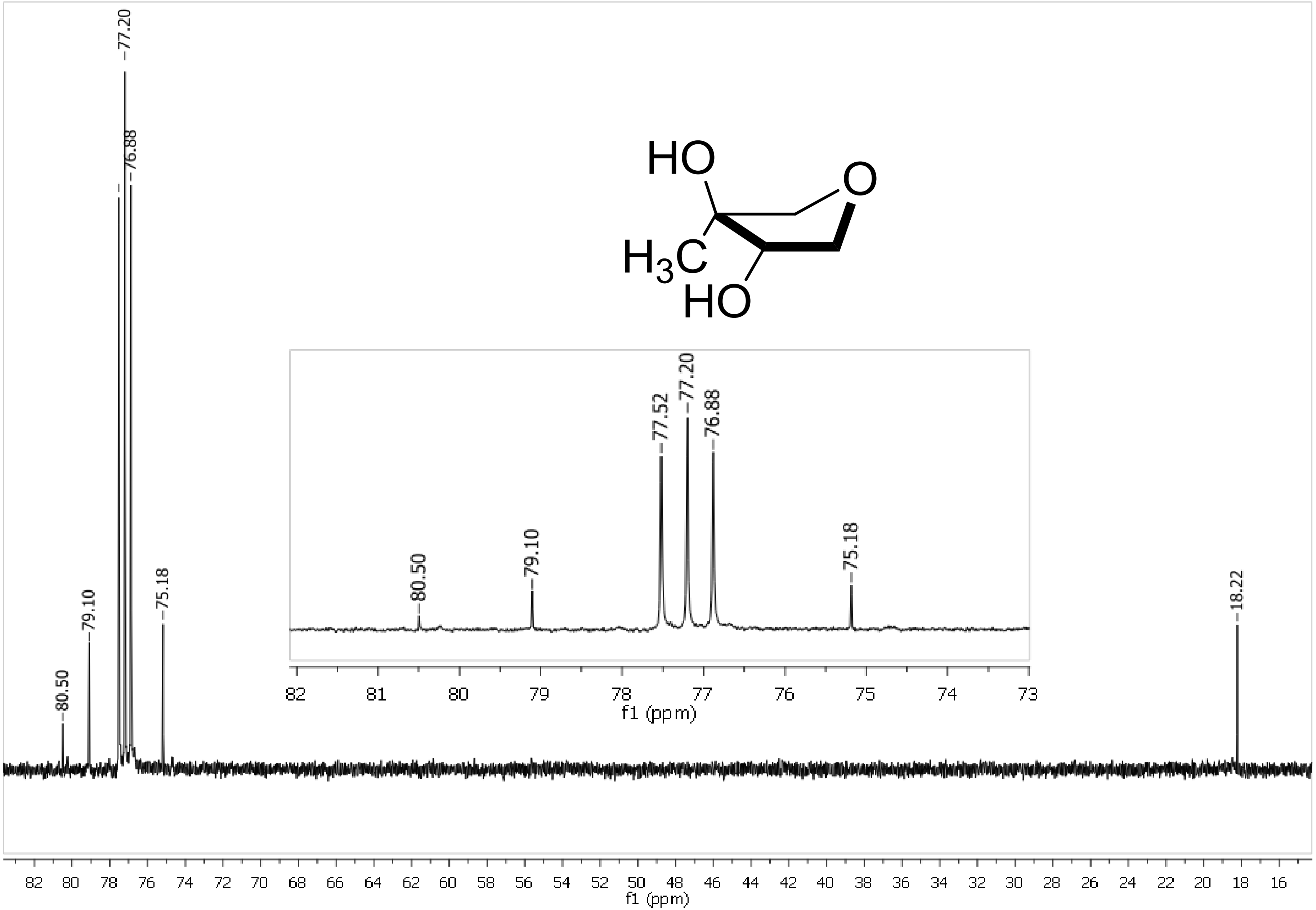

Figure S23. ^{13}C NMR (100 MHz, $CDCl_3$) of *trans*-3-methyltetrahydrofuran-3,4-diol (**15**).

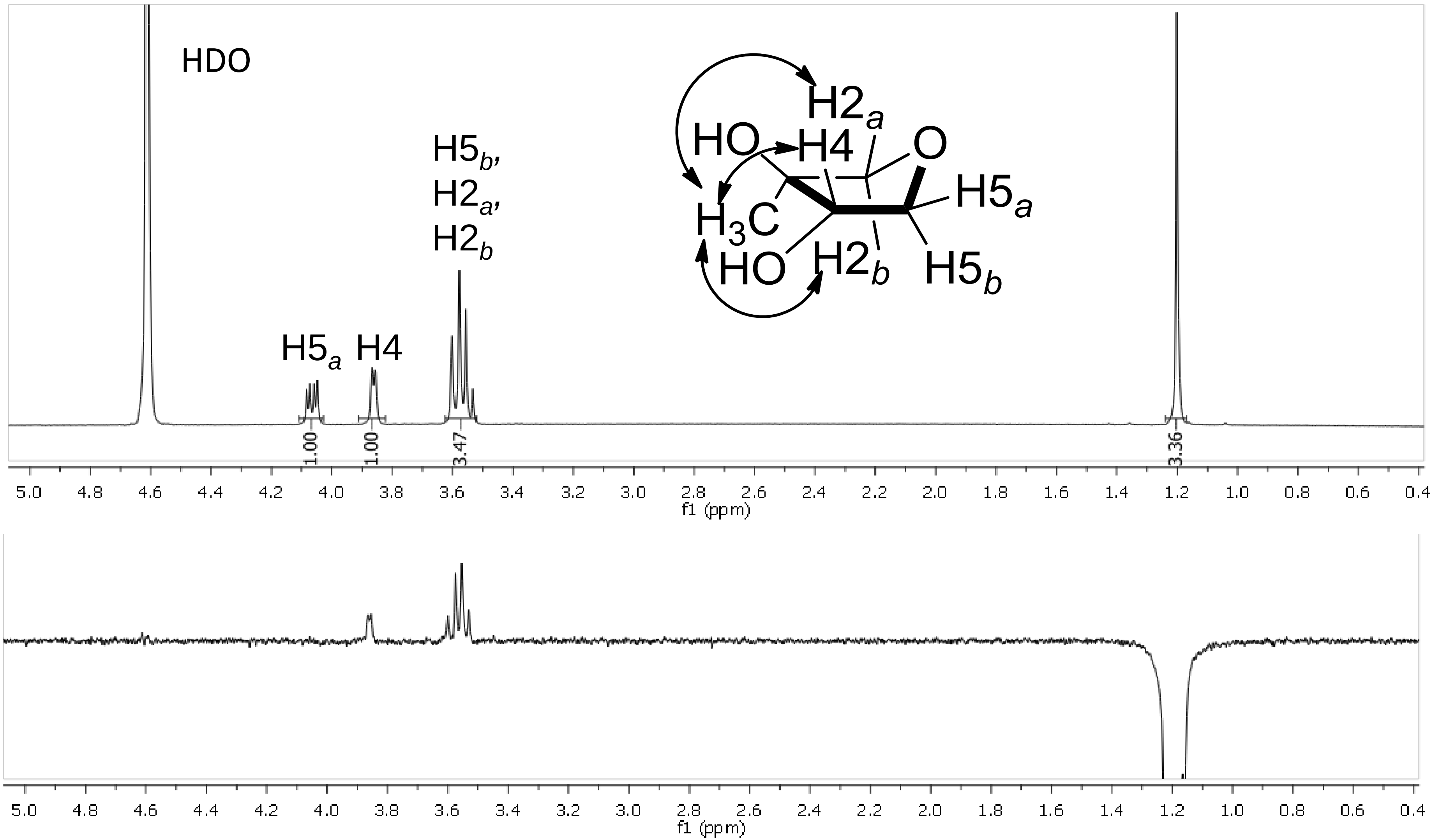

Figure S24. ^{1}H and NOESY 1D NMR (400 MHz, D_2O) of *trans*-3-methyltetrahydrofuran-3,4-diol (**15**). In contrast to the *cis*-isomer, irradiation of the methyl signal produces a much smaller enhancement of the H4 signal in the 1D NOESY spectrum (see Figure S21).

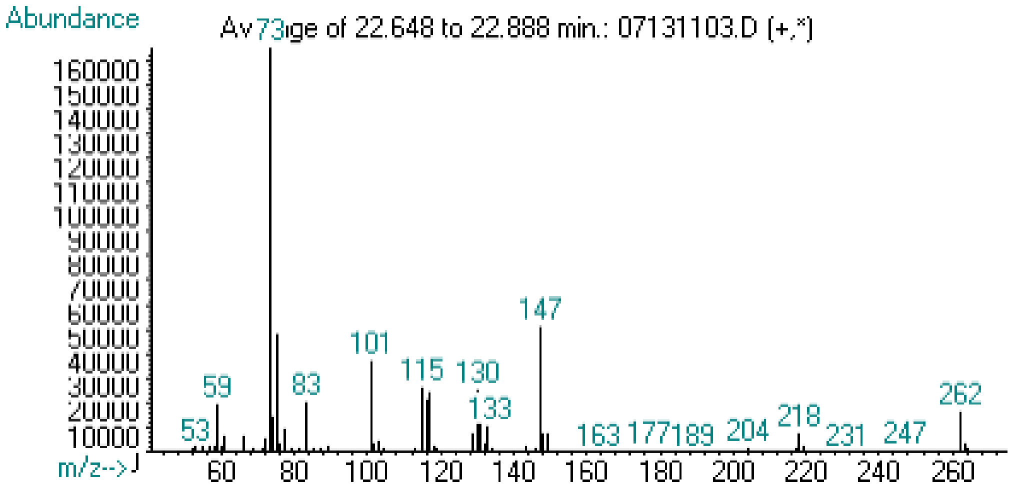

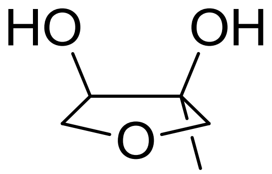

14

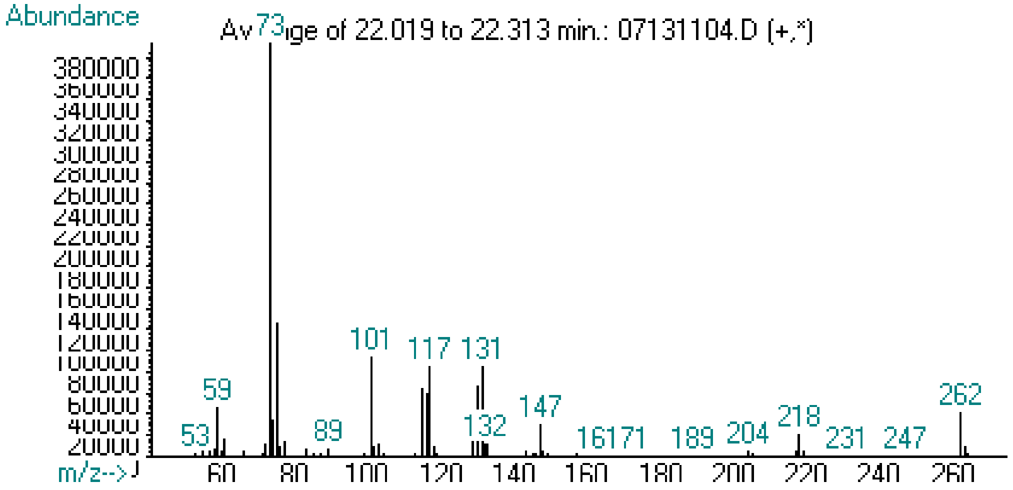

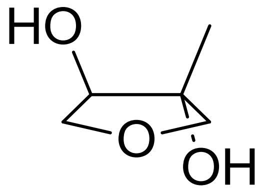

15

Figure S25. Positive GC-EIMS of *cis*-3-methyltetrahydrofuran-3,4-diol (**14**) and *trans*-3-methyltetrahydrofuran-3,4-diol (**15**).

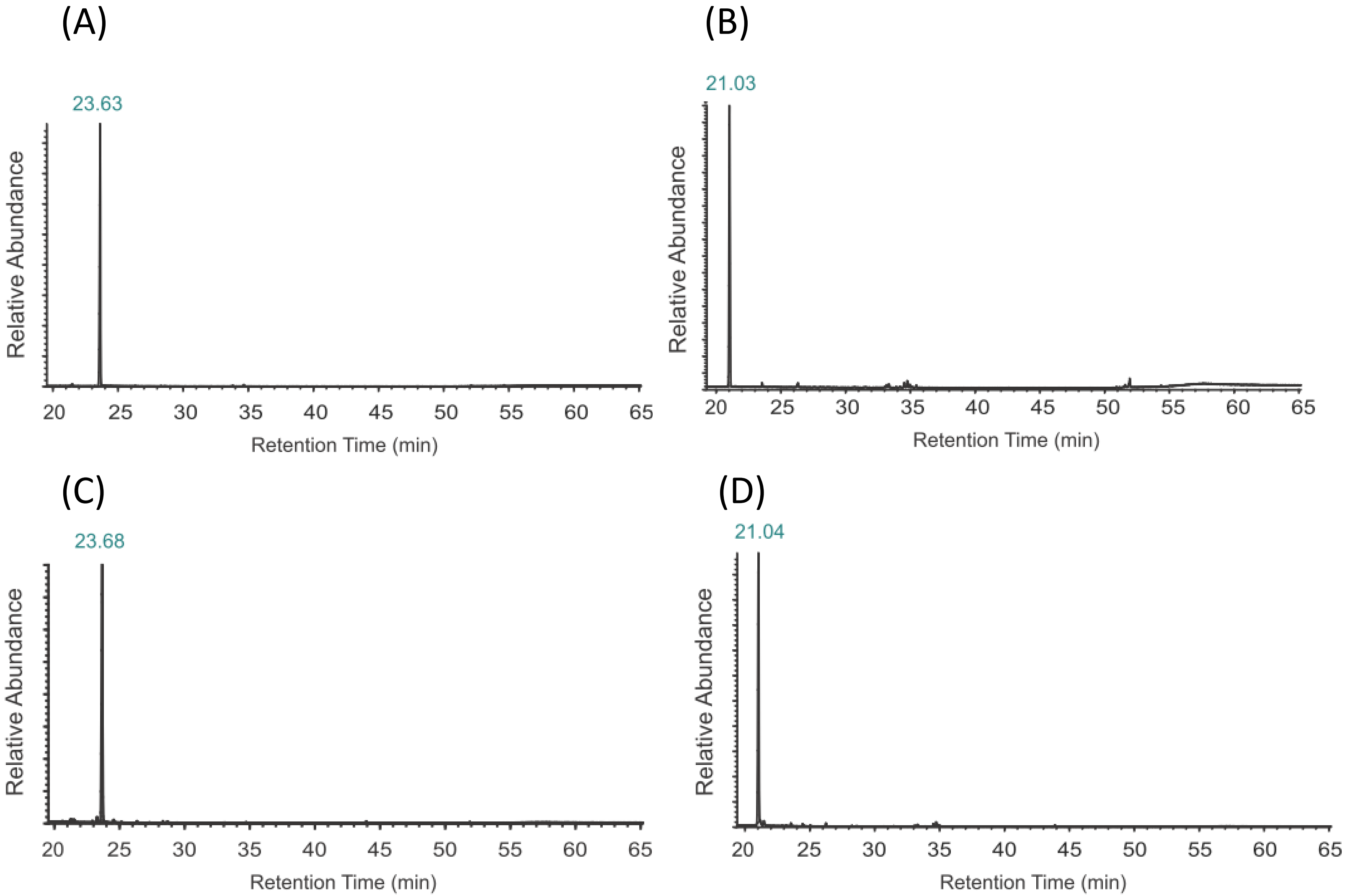

Figure S26. TIC from analysis of IEPOX isomers, 100 ng/µL in EtOAc : (A) and (B) freshly prepared IEPOX-3 and IEPOX-1, respectively; (C) and (D) the same solutions stored at -20 °C for 1 year.

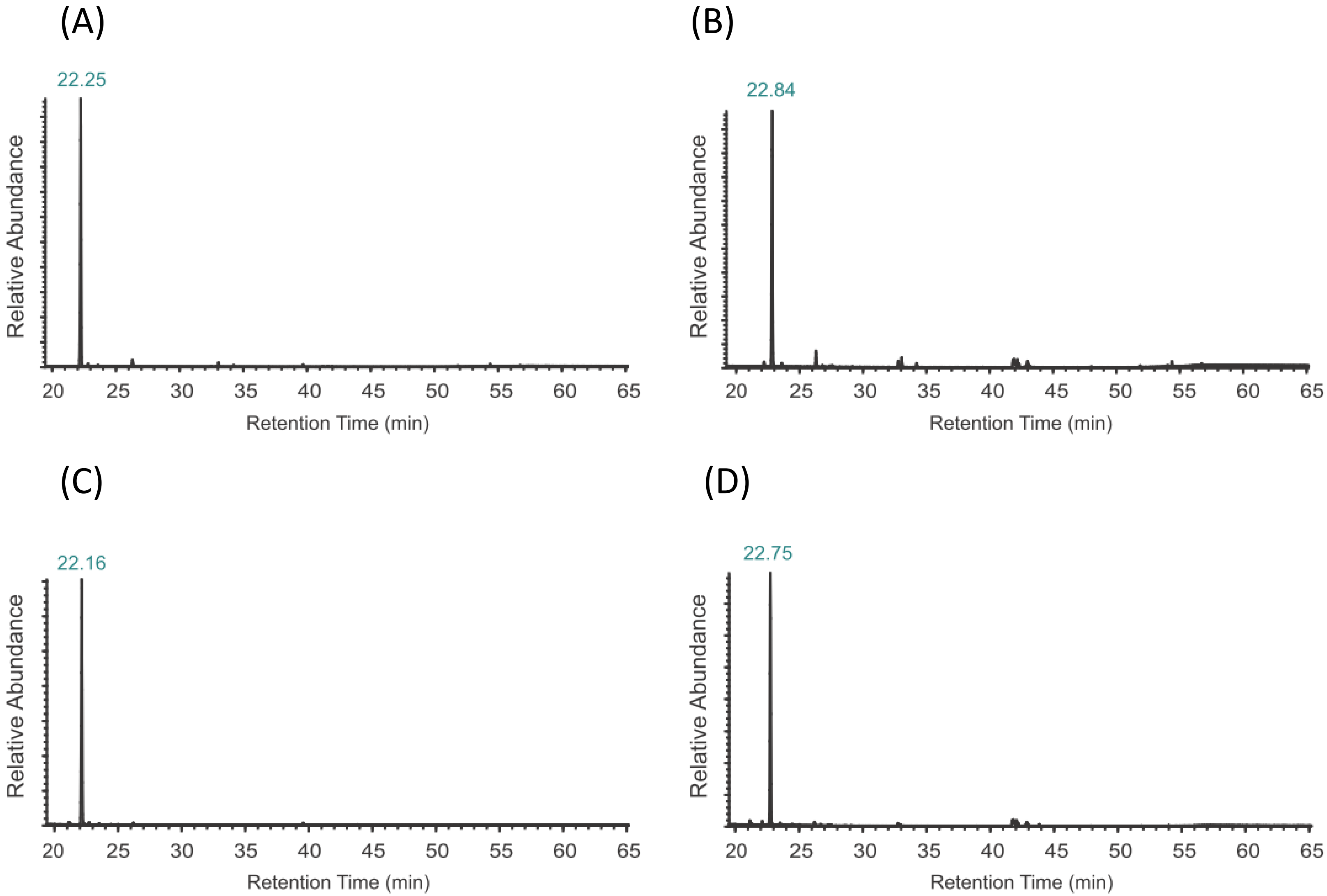

Figure S27. TIC from solutions of *trans*- and cis-MeTHF-3,4-diols, respectively, 100 ng/µL in ETOAc : (A) and (B) freshly prepared *trans*- and cis-MeTHF-3,4-diols, respectively; (C) and (D) the same solutions stored at -20 °C for 1 year.